Nuclear Instruments and Methods in Physics Research A 804 (2015) 59–63

Contents lists available at ScienceDirect

Nuclear Instruments and Methods in Physics Research A

journal homepage: www.elsevier.com/locate/nima

Study of pixel damages in CCD cameras irradiated at the neutron tomography facility of IPEN-CNEN/SP

R. Pugliesi *, M.L.G. Andrade, M.S. Dias, P.T.D. Siqueira, M.A.S. Pereira

Instituto de Pesquisas Energéticas e Nucleares, Centro do Reator de Pesquisas, Av. Prof. Lineu Prestes 2242, Cidade Universitária, 05508-000 São Paulo, Brazil

ARTICLE INFO

Article history:
Received 13 May 2015
Received in revised form
21 September 2015
Accepted 21 September 2015
Available online 30 September 2015

Keywords:
Neutron tomography
Neutron imaging
CCD sensor radiation damages

ABSTRACT

A methodology to investigate damages in CCD sensors caused by radiation beams of neutron tomography facilities is proposed. This methodology has been developed in the facility installed at the nuclear research reactor of IPEN-CNEN/SP, and the damages were evaluated by counting of white spots in images. The damage production rate at the main camera position was evaluated to be in the range between 0.008 and 0.040 damages per second. For this range, only 4 to 20 CCD pixels are damaged per tomography, assuring high quality images for hundreds of tomographs. Since the present methodology is capable of quantifying the damage production rate for each type of radiation, it can also be used in other facilities to improve the radiation shielding close of the CCD sensors.

1. Introduction

Neutron tomography is a three-dimensional imaging technique employed to study the internal structure of an object. A typical facility for tomography consists of a rotating table, a scintillator screen, a plane mirror and a CCD digital video camera. An important problem regarding these facilities is the high susceptibility of the CCD sensors to radiation damages which lead to a shortening of its lifetime as well as to a degradation of the captured image [1,2]. Besides the high cost of these cameras (usually they are the most expensive component of the facility), the worse the quality of the captured image, the worse the quality of the tomography [3]. Normally tomography facilities are installed at nuclear research reactors or at particle accelerators, and the radiation field around the CCD sensors can be quite different. The present work is focused in the facility installed at the research reactor of the Nuclear and Energy Research Institute (IPEN-CNEN/SP). In this case, fast and thermal neutrons as well as gamma rays are present.

A CCD image sensor consists of a silicon substrate with a large number of pixels arranged in a two-dimensional array. After being damaged by radiation, there may be a change in some operational parameters, resulting in malfunction and/or eventually a complete destruction of the sensor. The damages may be divided into two main kinds: surface and bulk damages. The first plays a minor role regarding such changes [4–6]. The second, which is the focus of the present work, is caused by the displacement of silicon atoms out of their lattice sites. These damages are induced by radiations which may transfer an energy higher than the displacement threshold around 20 eV to the Si atoms [7]. Neutrons can induce displacements either by elastic scattering, with threshold energy around 185 eV, or by neutron capture. In the latter case, the emitted prompt gamma ray yields a Si recoil atom with energy greater than 1 keV (which is much higher than the displacement threshold energy of 20 eV). On the other hand, further effects produced by thermal neutrons depend markedly on the activation of CCD and on the materials surrounding it [8,9]. The displacement induced by gamma rays is mainly due to electrons from photoelectric effect, Compton scattering or pair production. Gamma rays, with energies of some MeV, can produce secondary electrons mainly by Compton scattering with energies greater than 260 keV – the threshold for electrons to generate the displacements [4,5]. One of the consequences of damaged pixels is the appearance of permanent white spots superimposed to the image [1,2].

It is very important to mention that depending on the technology employed in their manufacturing, the CCDs can be differently affected by radiation. However, since all ordinary CCD sensors are susceptible to radiation damages, it is essential to protect them against radiation. For example in neutron tomography facilities, direct exposure of the CCD sensor to radiation is avoided by using a plane mirror to reflect the image generated in the scintillator. The reflected light impinges the camera located at 90° with respect to the radiation beam.

The purpose of the present paper is to present an overview of the methodology to evaluate damages in CCD sensors caused by

* Corresponding author.
E-mail address: pugliesi@ipen.br (R. Pugliesi).

http://dx.doi.org/10.1016/j.nima.2015.09.067
0168-9002/

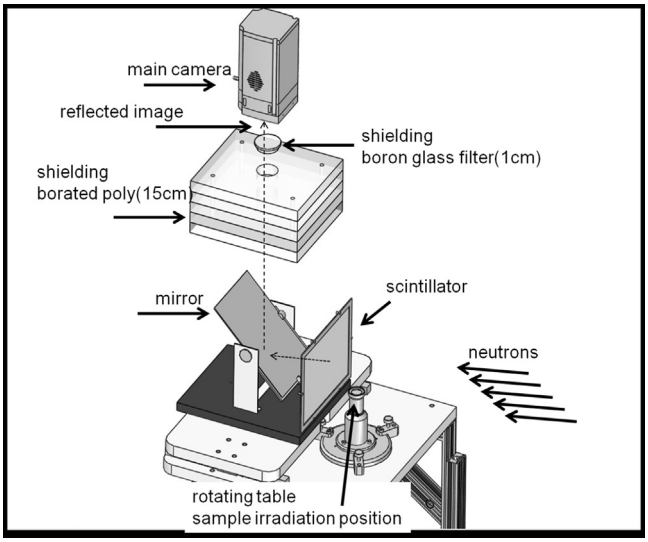

Fig. 1. Layout of the facility for neutron tomography of IPEN-CNEN/SP.

radiation beams at neutron tomography facilities, based on counting of white spots. In the first place, the damage production rate per radiation type is evaluated by making use of low cost CCD test cameras and, in the second place, these results are used to plan a safe experiment to evaluate the damages in the main camera CCD of the facility. The methodology was applied to the IPEN-CNEN/SP facility which, as described in reference [10], has already been optimized with respect to radiation protection of the CCD sensor.

2. Experimental procedure

The facility is installed at the radial channel #14 of the 4.5 MW, pool type, nuclear research reactor IEA-R1,[1] of the IPEN-CNEN/SP. It is a materials testing reactor, with a maximum thermal neutron flux around 1.0×10^{14} n cm^{-2} s^{-1} inside the core. The core consists of 24 fuel elements, enriched at 20% in U-235, surrounded by beryllium/graphite reflectors, and it is cooled by light water which acts also as neutron moderator and radiation shielding. The layout of the facility is shown in Fig. 1 and consists of a rotating table for sample irradiation, a 18×24 cm^2 ^{6}LiF(ZnS) – neutron scintillator screen, a 18×24 cm^2 glass based plane mirror, and an ANDOR digital video camera (model iKon-M) to image capture for the tomography (here referred as main camera). The camera provides 16 bit images, its CCD (1024×1024-pixel size 12×12 μm^2) is cooled and the shielding consists of borated poly plates 15 cm thick and a transparent boron glass filter 1 cm thick [10], as shown in the Fig.1. The characteristics of the radiation beam at the sample position are shown in Table 1.

The test cameras used in the present study were the standard ones used for surveillance and their main characteristics are shown in Table 2. They were irradiated at two different places: at the sample position and at the main camera position (see Fig. 1). The captured images were digitized in an 8 bit gray level scale using a PixelView capture frame grabber (model PV-CX850U-F) and an Optiplex 960 DELL computer. The counting of white spots was performed by the software Image-Pro Plus version 7.0 and included the whole image. The camera lenses remained covered by a cap in such a way that only the white spots were visible in the captured images. For the test cameras, a white spot was here defined as a pixel with gray level (GL) > 5. This value was determined analyzing histograms ($n°$ of pixels *vs* gray level) and counting pixels of captured images of several not-irradiated test cameras. The obtained results demonstrate that GL > 5 for less than 0.1% of the all pixels of the CCD. The intrinsic gray levels for 99.9% of the pixels arising from the manufacturing process of the CCD, ranged between 0 < GL < 5.

[1] IEA-R1. Denomination of the Nuclear Research Reactor installed at IPEN-CNEN/SP.

Table 1
Characteristics of the radiation beam at the sample position.

Parameter	Value
Thermal neutron flux (n cm^{-2} s^{-1})[a]	8×10^6
Fast neutron flux (n cm^{-2} s^{-1})	2.5×10^6
Gamma[b] dose rate (Sv h^{-1})	0.42[c]
Beam diameter (cm)	12

[a] Au-foil method.
[b] From U-235 fission and from structural materials of the reactor.
[c] Calculated by Monte Carlo simulation applying code MCNP version 5 [11].

Table 2
Characteristics of the test cameras.

Characteristics	Specification
Type	Intelbras-VM220DN
Image sensor	CCD Sony ¼ in.
Pixel size	9.6 μm(H) × 7.5 μm (V)
Number of active pixels	640(H) × 480(V)
Dimension of active area of the CCD	6.1 mm (H) × 3.6 mm (V)
Active area of CCD (cm^2)	0.22
Time/image (ms)	30

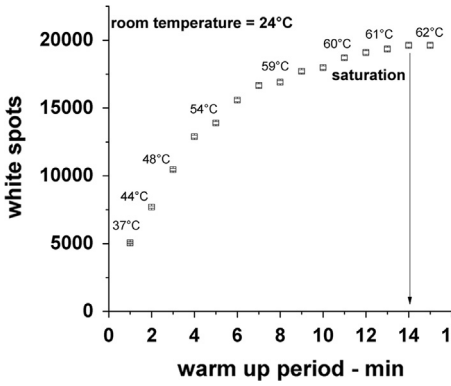

Fig. 2. Behavior of the number of white spots as a function of the warm-up period.

3. Data acquisition and analysis for the test cameras

3.1. Thermal equilibrium

Since the amount of visible white spots in a captured image depends of the temperature of the CCD [1], before starting the counting procedure it was necessary to determine the warm-up period, after the camera has been powered on, in order to reach thermal equilibrium. For such purpose, thermo-couples were fixed in some damaged CCDs of the test cameras, and they were powered on. As the temperature increases, images are captured and the white spots counted. For all the cameras, the obtained results were very close to each other and a typical one is shown in Fig. 2,

demonstrating that the CCDs reached the thermal equilibrium 14 min after the camera had been powered on, at a temperature of 62 °C, in a room temperature of (24.0 ± 0.2) °C. The uncertainties in the number of white spots (standard deviation in the number of counts) were about 1%.

3.2. Irradiation at the sample position

Three test cameras have been employed: *cam*(*a*) was irradiated in open beam; in this case, gamma-rays, fast and thermal neutrons will be able to induce damages; *cam*(*b*) was irradiated shutting the beam with a (Gd–Pb) shielding; in this case, gamma-rays and fast neutrons will be able to induce damages; *cam*(*c*) was irradiated shutting the beam with a (polyethylene-Gd-Pb) shielding; in this case, only gamma-rays may induce damages. Before the irradiation, the cameras were powered on for 14 min, the room temperature was (24 ± 0.2) °C, and one image of each camera was captured in order to establish the intrinsic background of white spots. The cameras were continued to be irradiated and after each period of 10 seconds one image was captured and the number of white spots as a function of the exposure time was registered. To separate the contribution due to each type of radiation, the following procedure has been established: gamma-rays correspond to the net number of spots in the image captured by cam(c); the contribution from fast neutrons was obtained by the net counting rate: [cam(b)–cam(c)]; the contribution from thermal neutrons was obtained by the net counting rate: [cam(a)–cam(b)]. The results for the number of white spots and associated uncertainties (one standard deviation) are shown in Fig. 3. A straight line was fitted by the least square method to each data set and the rates of white spots for each kind of radiation were evaluated from the slopes. The results were: $(314 \pm 26)\ s^{-1}$ for the fast neutron beam, $(91 \pm 4)\ s^{-1}$ for the thermal neutron beam and $(18 \pm 2)\ s^{-1}$ for the gamma-ray beam. Taking into account the neutron fluxes and the gamma dose rate shown in Table 1, 7.7×10^3 fast neutrons cm^{-2} or 8.8×10^4 thermal neutrons cm^{-2} or 7 μSv of gamma radiation are necessary to produce 1 white spot in the CCD. Considering the overall radiation field of the facility, and within the linearity range of Fig. 3, $(423 \pm 26)\ s^{-1}$ white spots are produced per second of exposure. Taking into account data from Tables 2, ~0.13% of the total active pixels are damaged per second, at the sample irradiation position.

3.3. Irradiation at 90° with respect to the beam

This experiment has a special interest because the test camera is positioned exactly where the main camera of the facility is installed. For this study, a single camera was employed which was irradiated in open beam. In this case, the radiations impinging the camera are: fast and thermal neutrons, as well as gamma-rays which are scattered by the scintillator, plane mirror, rotating table, air, etc., and attenuated by the radiation shield installed close to the camera lens (see Fig. 1) [10]. As described in the previous section, before irradiation the test camera was powered on for 14 min, the room temperature was maintained at (24 ± 0.2) °C, and one image has been captured in order to determine its intrinsic background of white spots. Since the intensity of the scattered radiation is very low, when compared to the intensity in the sample irradiation position, only one image, corresponding to an extended exposure time of 5 h was captured, to improve the counting statistics. The net number of white spots and its uncertainty (one standard deviation) was evaluated, resulting a damage production rate of $(1.2 \pm 0.2) \times 10^{-2}\ s^{-1}$. This value is ~35,000 times smaller than the rate at sample position (Section 3.2). This good condition is a result of the optimization performed in the facility in order to prevent damages in the main camera CCD sensor, as described in references [10,12].

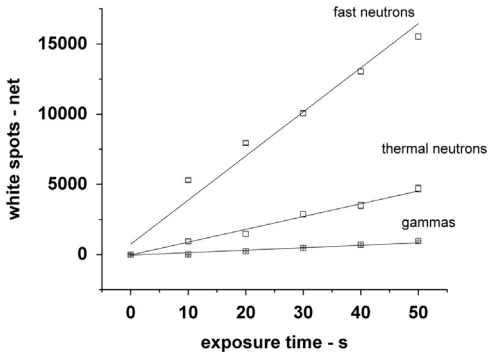

Fig. 3. Behavior of the white spots as a function of the exposure time, per radiation type.

Table 3
Summary of the results obtained for the test cameras.

Radiation	Parameter		
	Damage production rate sample position (s^{-1})	Damage production rate camera position (s^{-1})	Calculated damage production rate camera position (s^{-1})
Fast neutrons	314 ± 26	////////	$(1.0 \pm 0.2) \times 10^{-2}$
Thermal neutrons	91 ± 4	////////	$(1.5 \pm 0.4) \times 10^{-5}$
Gammas	18 ± 2	////////	$(1.2 \pm 0.1) \times 10^{-4}$
Total	(423 ± 26)	(1.2 ± 0.2) x 10^{-2}	$(1.0 \pm 0.2) \times 10^{-2}$

The damage production rates for each type of radiation were evaluated. For fast neutrons it was obtained by multiplying the corresponding damage production rate evaluated in Section 3.2, by the ratio of the fast fluxes at the camera position and at the at the sample position. However, since the flux at the main camera position is very low, the ratio between the fluxes was calculated by Monte Carlo simulation, applying code MCNP version 5 [11]. The obtained result was $(1.0 \pm 0.2) \times 10^{-2}\ s^{-1}$. The same procedure was employed for the thermal neutrons and for the gamma-rays, and the obtained results were $(1.5 \pm 0.4) \times 10^{-5}\ s^{-1}$ and $(1.2 \pm 0.1) \times 10^{-4}\ s^{-1}$ respectively. The damage production rate for the overall radiation field was $(1.0 \pm 0.2) \times 10^{-2}\ s^{-1}$. By comparing this overall rate with the one previously evaluated above of $(1.2 \pm 0.2) \times 10^{-2}\ s^{-1}$ is possible to conclude that they agree within their uncertainties and the damage production rates by thermal neutrons and gamma-rays are negligible. Therefore, fast neutrons are the main responsible for the damages. The results corresponding to Sections 3.2 and 3.3 are shown in Table 3.

3.4. Image quality

Fig. 4 (left) is a typical example of a captured image of a damaged CCD sensor of a test camera. Groups of individual white spots (Fig. 4 right) compose bright clusters and they are randomly distributed in the image. This effect produces localized discontinuities, leading to decrease in the image quality. The number of clusters is cumulative with the exposure. As a result, the discontinuities spread out to the whole image leading to a continuous degradation. According to these results, each cluster amounts 10–20 individual white spots, with gray levels ranging from 5 to 255, and covering areas between 700 and 1440 μm^2.

The relative decrease in the image quality, was evaluated by the change of mean gray level in the whole image caused by the

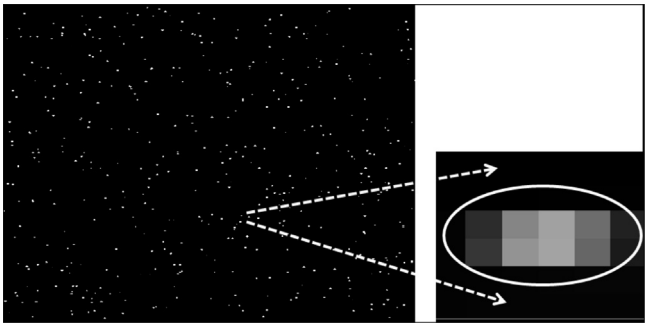

Fig. 4. Clusters of white spots in the captured image.

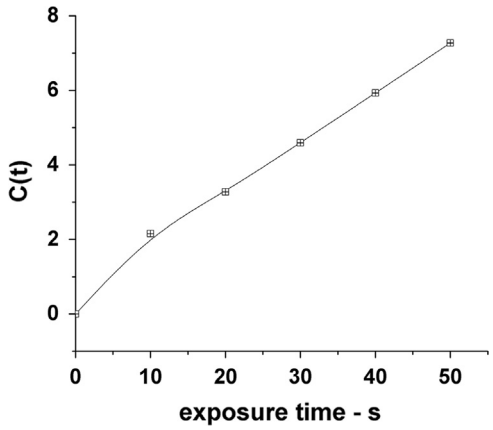

Fig. 5. Relative decrease in the image quality as a function of the exposure time.

clusters, as a function of the exposure time, and may be given by the following equation [13]:

$$C(t) = \frac{GL(t) - GL(0)}{GL(0)} \quad (1)$$

GL(t) is the mean gray level for exposure time t, and GL(0) is the mean intrinsic gray level ($t=0$). They were evaluated by averaging the gray levels of all pixels in the image applying the same software mentioned in Section 2. The experimental data was taken with a single test camera, which was also powered on for 14 min, at a room temperature of (24 ± 0.2) °C and irradiated in the sample position (see Fig. 1). GL(0) is the minimum achievable gray level value and the camera provides the best image quality. As the exposure time increases the amount of white spots, and consequently GL(t), increases too and image quality worsens according to Eq. (1). Fig. 5 shows the behavior of $C(t)$ for the present test camera in the $0 < t < 50$ s time range. The uncertainties in C (t) data were evaluated by usual error propagation applied to Eq. (1).

4. Data acquisition and analysis for the main camera

As mentioned in the introduction, depending of the technology employed in the CCD manufacturing, they may be affected differently by radiation [2,4,5]. Therefore, the results for the test cameras cannot be directly transferred to the main camera CCD. However, since the results obtained in Section 3.3 indicate very low damage production rate in the test cameras, it was possible to perform a safe and controlled experiment to evaluate, the damage production rate in the main camera of the facility. The camera lens was covered with a cap, as described in Section 2, and was positioned as shown in Fig. 1. The CCD temperature has been lowered to −20 °C and 5 images, each one captured during 1 second, before irradiating the camera. After that, the camera was irradiated in open beam for 500 s and other 5 images were captured. The temperature, the exposure time and the capture time per image, were selected because they are the typical ones to perform a tomograph in the present facility [10]. The counting of white spots, in these 10 images was performed by the same software previously employed in Section 3 and in the whole images.

Using the same criteria as described in Section 2, a white spot for this camera is defined as a pixel with gray level GL > 1400. By considering the net counting of white spots, the obtained damage production rate was $(2.4 \pm 1.6) \times 10^{-2}$ s^{-1} meaning that from 4 to 20 pixels of the CCD sensor are damaged per tomography. The high uncertainty is a consequence of the low exposure time.

The variation of image quality as a function of the exposure time was evaluated by Eq. (1). Here GL(0) and GL(500) are the average gray level values for the first 5 images and for the last 5 images, respectively, resulting GL(0)=(878 ± 0), GL(500)=(881 ± 1). Therefore, $C(t) \sim 0$ indicating a negligible image quality degradation per tomography.

5. Concluding remarks

According to the data from Sections 3.2 and 3.3, the tested CCD sensors are very susceptible to radiation damages, which are caused mainly by interactions with fast neutrons. As experimentally verified, the damage process is cumulative, but it is linear only for small exposure times [14].

Considering that damage production rate in test camera CCDs at the camera position was very low, it was possible to perform a safe and controlled experiment to evaluate the damages at the main camera of the facility.

The results for the main camera show that only 4–20 pixels of the CCD are damaged per tomography, demonstrating the high effectiveness of the measures that have been previously implemented in the facility to minimize radiation damages in its CCD sensor [10]. Furthermore, it is possible to conclude that the amount of damages created in the CCD, as well as the degradation of the image quality per tomography are negligible, assuring high quality images for hundreds of tomographs.

Although each tomography facility is unique in terms of neutron and gamma radiation fields, the proposed methodology applies for general shielding procedures, and may be employed by other users, in order to minimize the radiation damage rates at the CCD sensor of their main cameras. Thus high quality images can be achieved, for longer periods of use.

Acknowledgments

The authors are indebted to the International Atomic Energy Agency-IAEA, for partial financial support to this project, under the grant No. 17184, and also to the enterprise “Italvácuo-Comércio e Metalização em alto vácuo” which provided the metallization of the mirrors used in the present work.

References

[1] N. Bassler., Radiation and Environmental Biophysics 49 (2010) 373–378.
[2] A. Marbs, F. Boochs, Investigating the influence of ionizing radiation on standard CCD cameras and a possible impact on photogrammetric measurements. ISPRS Commission V Symposium'Image Engineering and Vision Metrology'-IAPRS V. XXXVI, vol. 5, 2006, pp. 25–27.
[3] Octopus 8.4 Manual, 2011. ⟨http://www.inct.be/en/software/octopus⟩.
[4] F. Hönniger, E. Fretwurst, G. Lindström, G. Kramberger, I. Pintilie, R. Röder, Nuclear Instruments and Methods in Physics Research, A 583 (2007) 104–108.

[5] G. Lindstroem, Nuclear Instruments and Methods in Physics Research, A 512 (2003) 30–43.
[6] G. Lindstroem, et al., Nuclear Instruments and Methods in Physics Research, A 465 (2001) 60–69.
[7] M. Moll. Radiation damage in silicon detectors-an introduction for non-specialists-CERN EP-TA1-SD Seminar, (2001).
[8] G.F. Knoll, Radiation Detection and Measurement, fourth ed., John Wiley & Sons, Inc., Hoboken, NJ, USA, 2010.
[9] W.J. Price, Nuclear Radiation Detection, second ed., McGraw – Hill, New York, NY, USA, 1964.
[10] R.M. Schoueri, C. Domienikan, F. Toledo, M.L.G. Andrade, M.A.S. Pereira, R. Pugliesi, Applied Radiation and Isotopes 84 (2014) 22–26.
[11] ORNL, Monte Carlo N-Particle Transport Code System, MCNP5, RSICC Computer Code Collection, Oak Ridge National Laboratory, Oak Ridge, TN, USA, 2006.
[12] M.A.S. Pereira, R.M. Schoueri, C. Domienikan, F. Toledo, M.L.G. Andrade, R. Pugliesi, Applied Radiation and Isotopes 75 (2013) 6–10.
[13] D. Okkalides, Physics in Medicine & Biology 44 (1999) N63–N68.
[14] C.J. Marshall, P.W. Marshall, CCD Radiation effects and test issues for satellite designers. NASA-GSFC Multi-Engineering Disciplinary Contract Task 1058, 2003.